Strong exciton-plasmon interaction in semiconductor-insulator-metal nanowires

Jie-Yun Yan*

School of Science, Beijing University of Posts and Telecommunications, Beijing 100876, China

(Received 16 May 2012; revised manuscript received 29 June 2012; published 16 August 2012)

The interaction of one-dimensional excitons and plasmons is theoretically investigated in semiconductor-insulator-metal nanowires. With the exact potentials presented analytically, the excitonic equation of motion in electron-hole-pair representation in real space is established. The optical properties of the system are derived by numerically calculating the evolution of the excitonic wave function. Linear absorption spectra demonstrate strong exciton-plasmon coupling in the nanostructures. The redshifts of the exciton absorption are found to be a result of interaction between the self-image potential and the indirect Coulomb interaction, of which the former brings the blueshift and the latter gives the redshift. The shifts reach the scale of 10 meV, which can be easily observed in experiment. Moreover, how the exciton-plasmon interaction is controlled by the parameters of the structure is also illustrated.

DOI: 10.1103/PhysRevB.86.075438 PACS number(s): 78.67.Uh, 71.35.Cc, 73.90.+f

I. INTRODUCTION

Nanomaterials incorporating semiconductor quantum structures and metamaterials have drawn a lot of attention in recent years. In these superstructures, the interaction between excitons in the semiconductor and neighboring plasmons in close metallic structures via the Coulomb coupling can significantly modify the optical properties of the otherwise single excitonic components. Many interesting phenomena have been found, such as Förster energy transfer,[1–3] the nonlinear Fano effect,[4,5] vacuum Rabi oscillations,[6–8] local field enhancement,[9–12] and enhancement and suppression of luminescence in different situations.[13–18] The prominent optical properties can be further controlled by changing the dielectric environment, sizes, shapes, interdistances, etc., which makes the hybrid excitons hot topics in the field of plasmonics.[19–22]

As far as the excitonic systems are considered, a large variety of semiconductor quantum structures are involved. The quantum wells in close proximity to metallic nanostructures[23–25] have been considered, which can provide the interaction between two-dimensional excitons and plasmons. Most research focuses on the systems including the semiconductor quantum dots, which generate zero-dimensional excitons. These kinds of excitons are usually taken as two-level systems under the external field. For example, the optical properties of superstructures composed of metal nanoparticles and semiconductor quantum dots have been intensively studied.[4,11,12,26–37] In the system, the exciton absorption shows redshift when accompanying the metal nanoparticles in most cases and the shift is on the order of 0.1 meV.[11] Compared with the quantum dots and quantum wells, the quantum wires exhibit their optical properties through the one-dimensional excitons (1D excitons) and possess the ability to propagate the electrons, holes, and photons along one direction, which makes them important building blocks in electrical or optoelectronic applications. Although 1D-exciton-plasmon interactions have also been studied for some cases,[38,39] how and in what degree the optical properties of the 1D excitons are modified by the coupled plasmons still deserve further investigations.

In this paper, we present a 1D-exciton-plasmon interaction system in semiconductor-insulator-metal nanowires. To our knowledge, the theoretical work for the optical properties in the system have not been considered, although the 1D nanowire providing the exciton-plasmon interaction has been synthesized in experiments.[40] 1D excitons in the excited semiconductor quantum wires (SQWs) of the system, strongly confined in the two-dimensional (2D) transverse space, will not only be dominated by the excitation fields, but also interplay with the plasmons in the metallic layers via the self-images of the created electrons and holes. However, the usual description of the excitons as dipoles seems difficult for analyzing the 1D-exciton-plasmon interaction, because the metal layer cannot create a resonant field enhancement on the dipoles aligning at the axis. To describe the optical properties of the 1D-exciton-plasmon interacting system, the equation of motion of the exciton wave function is established in the electron-hole-pair representation in real space. With a simplified model, the potentials felt by the electrons and holes contributed by the self-images are given analytically. Numerical results show that the exciton linear absorptions are strongly modified: They show redshifts, which are found to be a cooperation of two different effects caused by the interactions with the plasmons, and the shifts reach the order of 10 meV, which is far larger than that in the semiconductor quantum dots and metal nanoparticle systems. So the strong exciton-plasmon interaction can be observed easily in experiments. Moreover, we will also illustrate how the interaction of the exciton-plasmon interaction is controlled by size of the structure, distribution of the dielectric constant, energy band gap of the quantum wire, etc.

The paper is organized as follows. In Sec. II, the potentials of the electrons and holes in the SQWs are given analytically with a simplified model. The description of the optical properties of the system is presented in Sec. III. The numerical results are discussed in Sec. IV. Finally a brief conclusion is given.

II. ELECTRIC FIELDS INSIDE THE SYSTEM

The 1D-exciton-plasmon interacting system is modeled as a cylindrical SQW, infinite in the z direction, covered in order with a coaxial cylindrical insulator layer (IL) and a metal layer (ML), as shown in the upper part of Fig. 1. The outer radii of

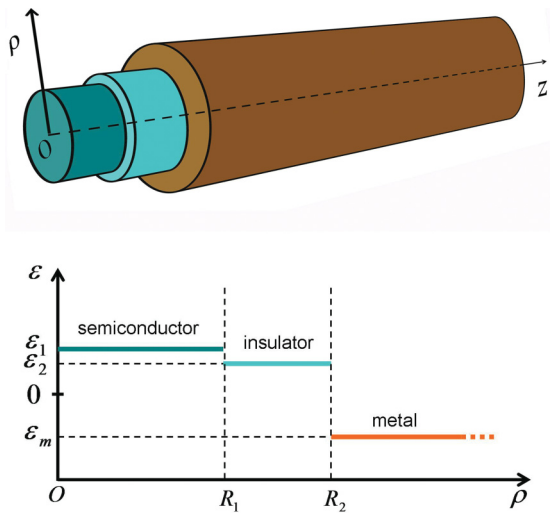

FIG. 1. (Color online) Upper: The structure of the semiconductor-insulator-metal nanowires infinite in the z direction. Lower: The distribution of dielectric constants along the ρ direction in the nanowires.

the SQW and the IL are denoted as R_1 and R_2, respectively. The lower part of Fig. 1 plots the distribution of the dielectric constants in the three-layer structure, where ϵ_1, ϵ_2 are those of the SQW and the IL, respectively, and $\epsilon_m(\omega)$ is the dielectric constant of the ML, depending on the frequency of the detecting optical field. Usually $\epsilon_m(\omega)$ is negative for the excitation near the band gap of typical SQWs. The ML is made of Au or Ag, as in most cases of the metal-incorporating complexes.

If the excitons in the SQW were excited, the created electrons and holes inside the SQW would induce their images (usually called self-images) in the IL and the ML because of the dielectric contrast. To highlight the exciton-plasmon interaction attributed to the existence of the ML and eliminate the possible dielectric confinement effect[41] contributed by the IL, we let the dielectric constant of the IL equal that of the SQW; i.e., $\epsilon_1 = \epsilon_2$. The self-images of electrons and holes, locating near the inner surface of the ML, bridge the interaction between the excitons in the SQW and plasmons in the ML. To simplify the theoretical description, we assume that the outer radius of the ML is infinity. This is reasonable if the ML is thick enough in comparison with the radial size of the SQW. In another words, the system can be taken as a common SQW but covered with an infinite-width metal layer rather than directly imbedded in the homogeneous dielectric background (i.e., $R_2 \to +\infty$, or called uncovered SQWs in the paper).

The main role of the IL is to prevent the electrons and holes excited out by the light in the SQW from experiencing the quantum tunneling to the outside in some degree. Here, we approximate the band gap of the IL as infinity and thus neglect the tunneling effect. In fact, the tunneling probability is small enough to be neglected when the insulator potential barrier is far beyond the SQW. The IL can also be made of wide band gap semiconductor materials, such as AlN with a direct band gap of 6.2 eV.[42] At the same time, the existence of the IL can avoid the unphysical behavior of the self-image potential to be mentioned later.

In these conditions, we can analytically express the potential created by an electron or hole inside the SQW. Suppose one particle with charge q' locates at $\boldsymbol{r'} = (\rho',\theta',z')$; the electrostatic potential at $\boldsymbol{r} = (\rho,\theta,z)$ should satisfy the Poisson equation

$$\Delta\Phi = -\frac{q'}{\epsilon_1}\delta(\boldsymbol{r}-\boldsymbol{r'}), \tag{1}$$

with the following boundary conditions:

$$\Phi_i|_{R_2} = \Phi_o|_{R_2}, \tag{2}$$

$$\epsilon_1 \frac{\partial\Phi_i}{\partial\rho}\Big|_{\rho=R_2} = \epsilon_m \frac{\partial\Phi_o}{\partial\rho}\Big|_{\rho=R_2}, \tag{3}$$

where Φ_i and Φ_o refer, respectively, to the potential $\Phi(\rho < R_2,\theta,z)$ and $\Phi(\rho > R_2,\theta,z)$. Actually the Coulomb potential $\phi_c \equiv \frac{q}{4\pi\epsilon_1}\frac{1}{|\boldsymbol{r}-\boldsymbol{r'}|}$ is just a particular solution to Eq. (1). According to the cylindrical symmetry of the system and homogeneity along the z direction, the potential has the form of $\Phi_i = \phi_c(\rho,\rho',\theta-\theta',z-z') + \phi_i(\rho,\rho',\theta-\theta',z-z')$ inside (in the dielectric environment of ϵ_1) and $\Phi_o = \phi_o(\rho,\rho',\theta-\theta',z-z')$ outside (in the ML), where $\phi_{i(o)}$ can be expanded as

$$\phi_{i(o)} = \frac{2}{\pi}\sum_{n=-\infty}^{+\infty}\int_0^{+\infty} dk e^{in(\theta-\theta')} \times [A_{i(o)}I_n(k\rho) + B_{i(o)}K_n(k\rho)]\cos k(z-z') \tag{4}$$

with constants $A(B)_{i(o)}$ determined by the boundary conditions (2) and (3). Here I_n and K_n are, respectively, the first and second kind of modified Bessel functions, and I_n' and K_n' are their derivatives correspondingly.

The Coulomb potential ϕ_c can also be expanded as

$$\phi_c = \frac{q'}{4\pi\epsilon_1}\frac{2}{\pi}\sum_{n=-\infty}^{+\infty}\int_0^{+\infty} e^{in(\theta-\theta')} \times I_n(k\rho_<)K_n(k\rho_>)\cos[k(z-z')]dk, \tag{5}$$

where $\rho_{<(>)}$ refers to the larger or smaller radial coordinate between ρ and ρ'. Finally we can find that the potential created by the charge q' gives the following constants:

$$A_i = \frac{q'(\epsilon_2-\epsilon_1)}{4\pi\epsilon_1}\frac{K_n(kR_2)K_n'(kR_2)I_n(k\rho_0)}{X_n(kR_2)}, \tag{6}$$

$$B_o = \frac{q'}{4\pi kR_2}\frac{1}{X_n(kR_2)}I_n(k\rho_0), \tag{7}$$

and A_o, B_i are zero. The function $X_n(x)$ is defined as

$$X_n(x) \equiv \epsilon_1 I_n'(x)K_n(x) - \epsilon_m I_n(x)K_n'(x). \tag{8}$$

If the ML is replaced by the material same as the SQW with dielectric constant ϵ_1, then the potential created by q' only includes the Coulomb potential of the point charge. Therefore the potential ϕ_i in the system is produced by the image of the charge q' in the ML. For a charge q located at $\boldsymbol{r}$, it would have the potential energy $V_c \equiv q\Phi_i = V_c^0 + V_c^S$, of which the first item is just the direct Coulomb interaction $V_c^0 = q\phi_c$ and the second is an indirect interaction with the help of the image of q', $V_c^S = q\phi_i$. We call the latter the indirect Coulomb interaction hereinafter.

For the charge q', besides interaction with another charged particle via the Coulomb interaction, it can also feel its own generated field. As the existence of the ML modifies the otherwise exclusive Coulomb potential of the charge, the additional self-energy of the charge at current position $\boldsymbol{r'}$ equals

$$U^S_{q'}(\rho') = \lim_{\boldsymbol{r}\to\boldsymbol{r'}} \int_0^{q'} \phi_i dq = \frac{q'}{2}\phi_i(\rho',\rho',0,0). \tag{9}$$

This is usually called the self-image potential, which can be explicitly expressed as

$$U^S_{q'}(\rho') = \frac{q'^2}{4\pi\epsilon_1} \sum_{n=-\infty}^{+\infty} \int_0^{+\infty} \frac{\epsilon_m - \epsilon_1}{\pi} \times \frac{K_n(kR_2)K'_n(kR_2)I^2_n(k\rho')}{X_n(kR_2)} dk. \tag{10}$$

From the above results, we can see that the potential of the electron and hole inside the SQW has been renormalized by the ML, where the field has also been influenced by the created electrons and holes. That is, the self-consistency of the field is included in the solved potentials. The self-consistency of fields is important for optical process in the low-dimensional nanostructures.[43]

III. LINEAR ABSORPTION OF THE EXCITON

When the system is radiated with an optical field with the electric field vector along the z direction, the Wannier exciton is excited in the SQW. Due to the confinement of the IL, the excitons are strongly localized in the two-dimensional potential of the quantum wire. The linear absorption of the SQW thus depends on the evolution of the electron-hole-pair wave function $\Psi(\boldsymbol{r}_e,\boldsymbol{r}_h,t)$, where $\boldsymbol{r}_i$ $(i = e,h)$ represents (ρ_i,θ_i,z_i) and $\rho_i \leqslant R_1$. Based on the symmetry of the system, we can assume[41]

$$\Psi(\rho_e,\rho_h,z,t) = \psi_e(\rho_e,t)\psi_h(\rho_h,t)\psi_z(z,t), \tag{11}$$

where z is the relative coordinate of the pair of electron and hole along the wire. Under this assumption, the electron-hole Coulomb interaction V^0_c and indirect Coulomb interaction V^S_c can be written as

$$V^0_c(\rho_e,\rho_h,z) = \frac{1}{4\pi\epsilon_1} \frac{-e^2}{\sqrt{(\rho_e-\rho_h)^2+z^2}}, \tag{12}$$

$$V^S_c(\rho_e,\rho_h,z) = \frac{-e^2}{4\pi\epsilon_1} \int_0^{+\infty} \frac{2(\epsilon_m-\epsilon_1)}{\pi} C\cos kz dk, \tag{13}$$

where the factor C reads

$$C \equiv \frac{K_0(kR_2)K'_0(kR_2)I_0(k\rho_e)I_0(k\rho_h)}{X_0(kR_2)}. \tag{14}$$

Here we consider the screened Coulomb interaction with a constant dielectric function; thus the influence of retarded interaction[44,45] is beyond our consideration.

In the effective-mass approximation and real-space representation, the wave function obeys an inhomogeneous Schrödinger equation:

$$i\hbar(\partial_t + g_2/\hbar)\psi(\rho_e,\rho_h,z,t) = H\psi(\rho_e,\rho_h,z,t) - d_{cv}E(t)\delta(\boldsymbol{r_e}-\boldsymbol{r_h}), \tag{15}$$

with the initial condition

$$\Psi(\rho_e,\rho_h,z,-\infty) = 0, \tag{16}$$

where d_{cv} is the interband dipole matrix element and g_2 is the interband dephasing rate. The Hamiltonian is

$$H = H_0 + V^0_c(\rho_e,\rho_h,z) + V^S_c(\rho_e,\rho_h,z) + U^S_e(\rho_e) + U^S_h(\rho_h), \tag{17}$$

where

$$H_0 = -\frac{\hbar^2}{2m^\perp_e}\nabla^2_{\rho_e} - \frac{\hbar^2}{2m^\perp_h}\nabla^2_{\rho_h} - \frac{\hbar^2}{2\mu}\nabla^2_z, \tag{18}$$

and μ is the reduced mass of the electron-hole pair $\mu = (1/m^\parallel_e + 1/m^\parallel_h)^{-1}$, and $m^\parallel_{e(h)}$ is electron (hole) effective masses in the z direction and $m^\perp_{e(h)}$ in the $\boldsymbol{\rho}$ plane. The center-of-mass motion of the electron-hole pair is neglected. $U^S_{e(h)}$ is the self-image potential of the electron (hole). As we want to find the linear absorption of the system in stationary condition, we assume that the electron-hole wave funtion oscillates with relatively static amplitude and the created electrons and holes feel a quasistatic potential. Thus the eletrostatic potential obtained before is used here.

The interband polarization is

$$P(t) = \frac{1}{V}\int_0^{+\infty} d^*_{cv}\Psi(\rho,\rho,z=0,t)2\pi\rho d\rho \tag{19}$$

and the optical absorption spectrum is

$$\chi(\omega) = \mathrm{Im}\left[\frac{P(\omega)}{E(\omega)}\right], \tag{20}$$

where $P(\omega)$ and $E(\omega)$ are the Fourier transformations of $P(t)$ and $E(t)$, respectively. The equation can be solved with the finite-difference time-domain method in real space,[46–49] and the optical absorption is obtained by fast Fourier transformations.

When the absorption of the system was considered as a whole, the contribution by the ML should also be taken into account. However, in the exciton-plasmon interaction system, the absorption of the metal only provides a relatively smooth background as compared with that of the excitons, especially when the excitons are far from resonance with the plasmon peak.[11] Therefore we put the emphasis on the absorption of the hybrid excitons in the SQW in the work.

IV. RESULTS AND DISCUSSION

First, we calculate the exciton absorption in a typical set of parameters to discuss the role of the potential $U^S_{e(h)}$ and V^S_c. The inner radius and outer radius of the IL are chosen as $R_1 = 40$ nm and $R_2 = 50$ nm, respectively. The electronic effective mass is $m^{\parallel,\perp}_e = 0.067m_0$, where m_0 is the free electron mass. Our theory is applicable to both heavy-hole and light-hole excitons, but only the former is focused on here. The effective masses parallel and perpendicular to the z direction of the heavy holes are respectively expressed as $m^\parallel_h = (\gamma_1+\gamma_2)^{-1}m_0$ and $m^\perp_h = (\gamma_1-2\gamma_2)^{-1}m_0$, with the Luttinger parameters $\gamma_1 = 6.85$ and $\gamma_2 = 2.1$ for GaAs material. The band gap of the uncovered SQWs is 1.5 eV. The dielectric constant ϵ_1 is set as $10\epsilon_0$ (ϵ_0 is the vacuum dielectric

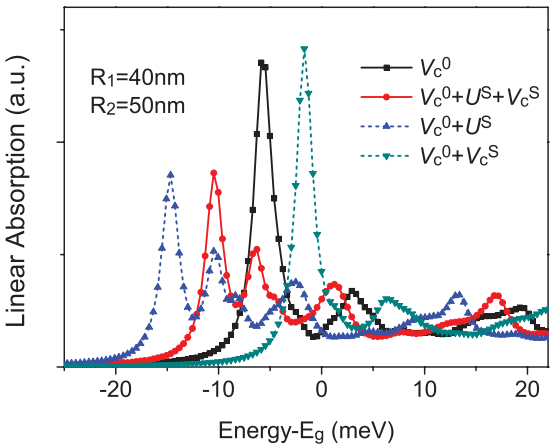

FIG. 2. (Color online) The linear absorptions of the system with four different Hamiltonians $H = H_0 + H_x$, where the detailed expression of H_x for corresponding lines are listed in the legend. Used parameters are stated in the context.

constant). The ML is made of Au, whose dielectric constant ϵ_m is about $-25.9\epsilon_0$ for the photonic energy near the band edge excitation. In this paper the dielectric constants of metals are taken from the Ref. 50. The dephasing rate g_2 is 1 meV for a clear spectral resolution. The dipole matrix element d_{cv} is 0.7 nm/e.

Besides the kinetic energies of the electron and the hole, the parts of potentials V_c^0, $V_c^0 + U^S + V_c^S$ (U^S refers to $U_e^S + U_h^S$), $V_c^0 + U^S$, and $V_c^0 + V_c^S$ are in turn included in the Hamiltonian for calculations. The linear absorption spectra of the SQWs under these four cases are shown in Fig. 2. The case of V_c^0 is just the linear absorption of the uncovered SQWs imbedded in the same dielectric environment. The lowest excitonic absorption peak locates at about 5 meV below the band gap in this case. The case of $V_c^0 + U^S + V_c^S$ gives the absorption of the 1D-exciton-plasmon interaction system. It is clear that both the line shape and peaks' positions are changed. To analyze the respective influences of these potentials, we calculate the absorptions with U^S and V_c^S added separately. Comparing the case of $V_c^0 + V_c^S$ with that of V_c^0, we can see that the indirect Coulomb interaction V_c^S counteracts the Coulomb interaction V_c^0, leading to reduced excitonic binding energy. The conclusion can also be drawn from the analysis of the formulas (13) and (14), of which the factor $X_n(kR_2)$ in the integrand is negative. When all the factors are considered, the potential V_c^S finally behaves as a positive and repulsive potential, totally different from V_c^0, a negative and attractive one. If the ML is substituted by materials with dielectric constants $\epsilon_m > 0$, the factor $X_n(kR_2)$ is then always positive, leading to $V_c^S > 0$ and increasing binding energy. Therefore the repulsive indirect Coulomb interaction V_c^S is the characteristics of the SQWs covered with MLs.

The influence of the potential $U_{e,h}^S$ is relatively complex. By comparing the absorption under the case of $V_c^0 + U^S$ and V_c^0, it is found that U^S causes a redshift of the lowest excitonic peak. The potential U^S is drawn in Fig. 3(b) under the same parameters. It presents two features: (1) negative both for electrons and holes; (2) higher in the center and lower at the edge of the SQW. Undoubtedly the first one would lower the excitonic energy levels. The second would cause the electrons and the holes to

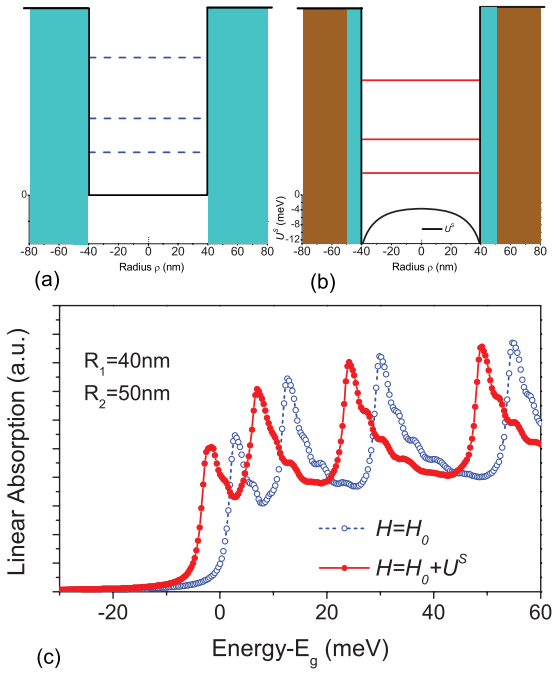

FIG. 3. (Color online) (a) Schematics of energy levels and confinement potential in the uncovered SQWs. (b) Schematics of the changed energy levels and confinement potential in the SQW-IL-ML system, with the accurate potential U^S plotted. (c) The linear absorptions calculated with the Hamiltonians $H = H_0$ (hollowed circle line) and $H = H_0 + U_e^S + U_h^S$ (solid circle line). Parameters are the same as in Fig. 2.

prefer to move centrifugally. That means the confinement in the $\boldsymbol{\rho}$ plane is weakened, or equivalently the electrons and the holes are delocalized by the potential to some extent, which results in the enlargement of the effective radius of the quantum wire and thus drops in the energy levels. In a word, the potential U^S results in the redshift of the excitonic levels. This is reasonable because the considered charges inside the SQW are attracted by their self-images, which have opposite charges because of the metal materials. The schematics of the confinement potentials for uncovered SQWs and the SQW-IL-ML system are drawn in Figs. 3(a) and 3(b) for a vivid illustration. It is worth mentioning that the divergency of the potential at the $\rho = R_2$ is avoided by the existence of the IL. The physical meaning is that the charge inside the SQW can never meet its image in the ML for the infinite potential barrier.

The role of potential U^S can also be seen from the comparison of absorption spectra calculated by two different Hamiltonians: $H = H_0$ and $H = H_0 + U_e^S + U_h^S$. The former is actually the continuum absorption of uncovered SQWs without excitonic effect. The results are shown in Fig. 3(c). The characteristics of the 1D exciton energy levels is evident in the absorption spectra. The added potential $U_{e,h}^S$ really makes the band edge an obvious redshift. However, the wave function of the excitons in this case is modified by the irregular potential after all; the absorption line shape is changed consequently. To sum up, the absorption of the 1D-exciton-plasmon system is the cooperation of the blueshift-inducing indirect Coulomb potential and the redshift-inducing self-image potential. Quantitatively, the final redshift shows that

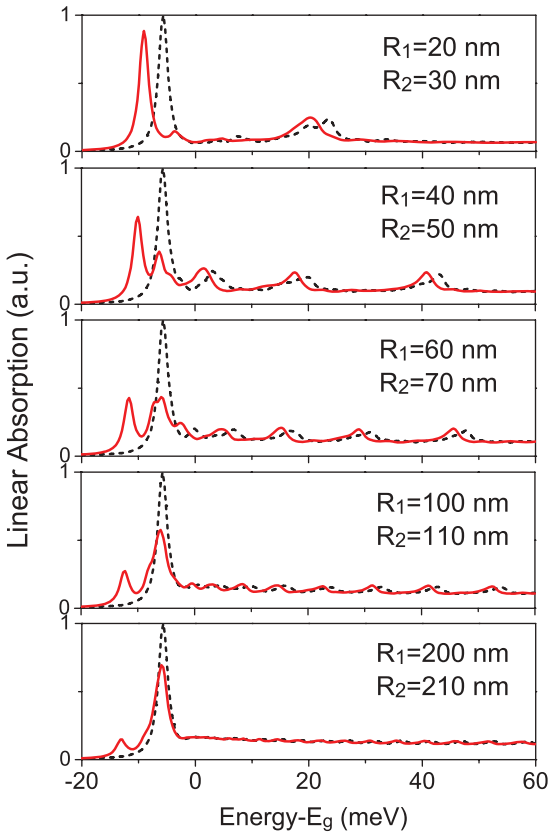

FIG. 4. (Color online) The absorption spectra of the semiconductor-insulator-metal nanowires with R_1 changing while $R_2 - R_1$ is unchanging. The absorptions of uncovered SQWs (or only the potential V_c^0 considered) are plotted with dashed lines for comparison for each spectrum.

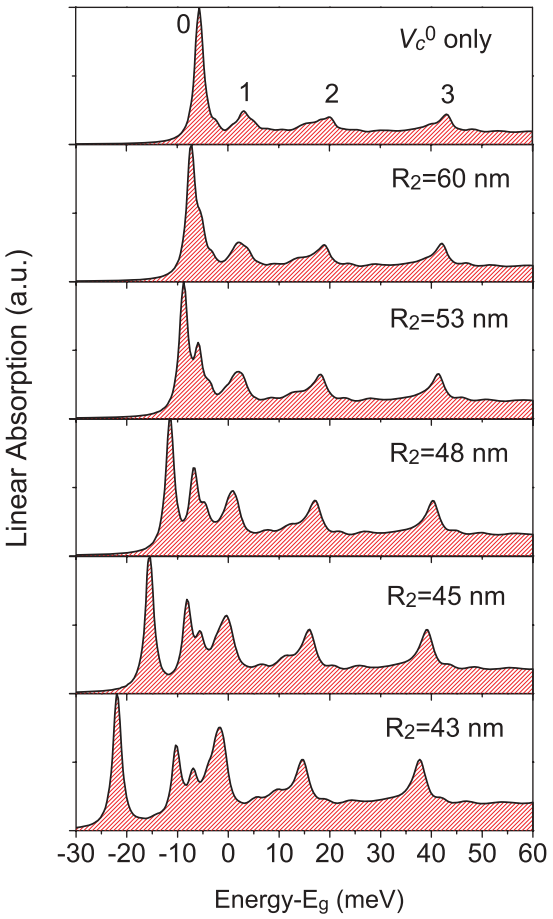

FIG. 5. (Color online) The absorption spectra of the semiconductor-insulator-metal nanowires with $R_1 = 40$ nm and R_2 changing from 60 nm to 43 nm. The absorption calculated with Hamiltonian $H = H_0 + V_c^0$ is also given on the top for reference.

the indirect Coulomb interaction $V_c^S(\rho,\rho,0)$ plays a leading role. We notice that the item with $n = 0$ in $U_e^S(\rho) + U_e^S(\rho)$ equals the value of $V_c^S(\rho,\rho,0)$, which gives us some intuitive understanding of why the redshift is stronger than the blueshift when both U^S and V_c^S are added.

To demonstrate the evolution of linear absorption with the radius of the SQW, we change R_1, R_2 while keeping $R_2 - R_1 = 10$ nm and get the spectra plotted in Fig. 4. The other parameters are unchanged. Under each group of radii, the absorptions with the Hamiltonians $H = H_0 + V_c^0 + U^S + V_c^S$ (spectrum B, red solid lines) and $H = H_0 + V_c^0$ (spectrum A, black dashed lines) are calculated. The spectra are normalized to their maximum value of spectrum A for each group. The higher discrete exciton levels get more and more close and finally disappear when the radius R_1 increases, which implicates the transformation from 1D exciton to the 3D exciton. The lowest excitonic peak in spectrum B when $R_1 = 20$ nm is modified most seriously. With the radius increasing, the new peak diminishes gradually and finally becomes a small side peak at the redshift side of the original exciton ground absorption. This is because the electrons and holes close to the axis in the SQWs have negligible influence from their images when the radius becomes large enough, and therefore the modification of the exciton absorption is relatively weak. However, the potentials U^S near the surface of the SQW $\rho = R_1$ for the different systems have almost the same value, which explains the almost same position of the new lowest exciton peaks.

It is evident that the distance between the electrons or holes and their images is an important factor determining the strength of interaction between excitons and plasmons. Now we observe the change of absorption by decreasing the parameter $R_2 - R_1$ while keeping the radius of the SQW fixed; i.e., $R_1 = 40$ nm. The value of $R_2 - R_1$ is actually the width of the potential barrier, determining the interaction distance. The limitation of $R_2 = +\infty$ is just the single metal-uncovered SQW. The absorption spectra are shown in Fig. 5, where the spectra with $R_2 = 60$ nm, 53 nm, 48 nm, 45 nm, and 43 nm are displayed in order. The linear absorption of the uncovered SQW (or R_2 is big enough) is also given for comparison, from which we can clearly distinguish the exciton absorption peak of different subbands, which from left (low energy) to right (high energy) are labeled as 0, 1, 2, 3, ... The absorptions of the high-order-subband excitons appear Fano line shaped due to the discrete exciton energy level locating at the continuums of the lower subbands. All the spectra are normalized to each maximum of theirs. With the decreasing of R_2, the peaks 1, 2, and 3 show redshifts and increasing

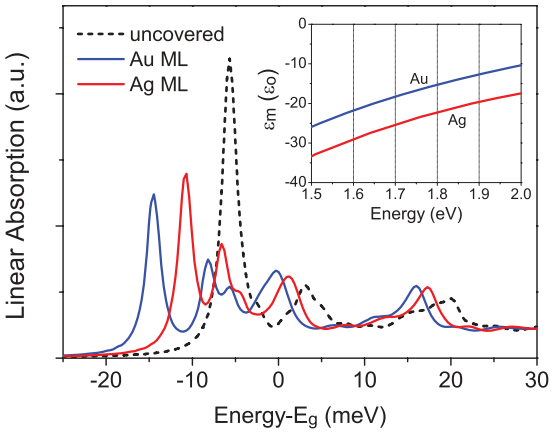

FIG. 6. (Color online) The absorption spectra of the semiconductor-insulator-metal nanowires ($R_1 = 40$ nm and $R_2 = 50$ nm) for different metal materials: Au and Ag. The band gap of the corresponding uncovered SQWs is 1.8 eV, whose absorption is plotted with dashed line. Inset draws the functions of dielectric constants of Au and Ag.

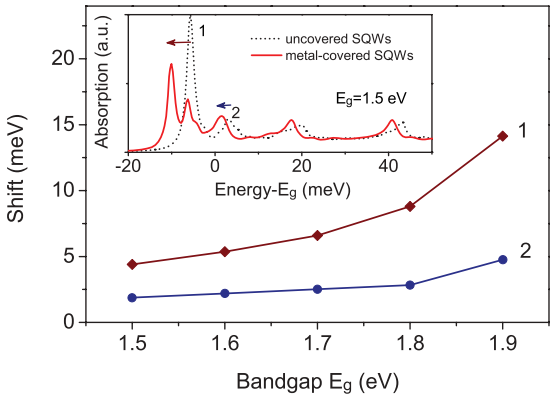

FIG. 7. (Color online) The shifts of the absorption peaks for systems with SQWs of different band gaps, changing from 1.5 to 1.9 eV by step 0.1 eV. The absorption spectra for the value of 1.5 eV are given in the inset and the corresponding absorption peaks are labeled with 1 and 2, respectively.

strengthes relatively. The most outstanding change is the lowest exciton absorption peak 0. It is split first, and then more and more new peaks are generated in the redshift direction. If the main absorption of the system is considered, a totally distinguishable redshift on the order of magnitude of about 10 meV can be detected. The shift is about 100 times stronger than that in the zero-dimensional exciton-plamson interaction system.[11]

Besides the width of potential barrier, the dielectric contrast between the SQW and the ML also has a key influence on the optical properties of the 1D exciton-plasmon system. First, we discuss the effects caused by different metal materials. Figure 6 gives the absorptions of the SQW-IL-ML system with the ML made of Au and Ag, whose dielectric constants are $-15.3\epsilon_0$ and $-22.3\epsilon_0$, respectively, under the same excitation with photonic energy 1.8 eV. The exciton absorptions of these two cases have different shifts in comparison with the metal-uncovered SQWs. It is evident that the excitons interplaying with the plasmons in the Au causes a bigger redshift on the lowest peak.

As the dielectric constant of metals ϵ_m is sensitive to the frequency of the excitation, as shown in the inset of Fig. 6, exciton absorption of the system would also experience different shifts when the frequency of the optical field changes. Because the photonic energy of the laser detecting the exciton absorption locates near the band gap of the SQWs, the dielectric constants of the ML is determined by the band gap of the SQWs. We investigate the absorptions of the SQW-IL-ML nanowires with $R_1 = 40$ nm and $R_2 = 50$ nm by tuning the band gap of the SQWs from 1.5 eV to 1.9 eV with step 0.1 eV. The spectra for a typical value of $E_g = 1.5$ eV are plotted in the inset of Fig. 7. The same as we analyzed before, the original absorption labeled with 1 for the metal-uncovered SQWs is split and the lowest absorption peak has an apparent redshift, while other higher exciton absorptions such as the peak labeled with 2 experience redshifts in varying degrees. Increasing redshifts of these peaks are observed with the band gap energy increasing, as Fig. 7 shows. The shift exceeds 10 meV for the case of $E_g = 1.9$ eV. The result can also be explained by the ever-increasing $X_n^{-1}(\cdots)$ in the formula of the potentials. Actually there exists a singularity for the factor when the ϵ_m increases further. We find that the redshift of the lowest exciton absorption can even exceed 40 meV with the dielectric constant ϵ_m fixed at $-10\epsilon_0$. The adjustable exciton absorption in the scale of 10 meV is undoubtedly useful in the optoelectronic applications.

V. CONCLUSION

We studied the optical properties of 1D-exciton-plasmon interaction system in the semiconductor-insulator-metal nanowires. The equation of motion for the excitons in the electron-hole-pair representation in real space is established, with the exact potentials felt by the excitons presented analytically. The linear absorption of the system is obtained by calculating the evolution of the excitonic wave function. We found that the lowest exciton absorptions show redshifts on the order of 10 meV, large enough to be easily observed in experiment when compared with the quantum dots/metal nanoparticles complexes. Through the analysis of the numerical results, we revealed that the redshift is underlaid by two competing factors: the self-image potential causing redshift and indirect Coulomb interaction resulting in blueshift. We also illustrated how the optical properties determined by the exciton-plasmon interaction are influenced by the radius of the SQWs, dielectric constant of the ML, width of the IL, and excitation energy.

ACKNOWLEDGMENTS

This work is supported by the National Natural Science Foundation of China (Grant No. 11004015), the Doctoral Fund of the Ministry of Education of China (Grant No. 20100005120017), and the National Basic Research Program of China (Grant No. 2010CB923200).

*jyyan@bupt.edu.cn

[1] J. N. Farahani, D. W. Pohl, H.-J. Eisler, and B. Hecht, Phys. Rev. Lett. **95**, 017402 (2005).

[2] S. M. Sadeghi and R. G. West, J. Phys.: Condens. Matter **23**, 425302 (2011).

[3] A. O. Govorov, J. Lee, and N. A. Kotov, Phys. Rev. B **76**, 125308 (2007).

[4] W. Zhang, A. O. Govorov, and G. W. Bryant, Phys. Rev. Lett. **97**, 146804 (2006).

[5] W. Zhang and A. O. Govorov, Phys. Rev. B **84**, 081405 (2011).

[6] H. T. Dung, L. Knoll, and D.-G. Welsch, Phys. Rev. A **62**, 053804 (2000).

[7] G. S. Agarwal and S. V. ONeil, Phys. Rev. B **28**, 487 (1983).

[8] V. V. Klimov, M. Ducloy, and V. S. Letokhov, Phys. Rev. A **59**, 2996 (1999).

[9] K. T. Shimizu, W. K. Woo, B. R. Fisher, H. J. Eisler, and M. G. Bawendi, Phys. Rev. Lett. **89**, 117401 (2002).

[10] H. Mertens, J. S. Biteen, H. A. Atwater, and A. Polman, Nano Lett. **6**, 2622 (2005).

[11] J.-Y. Yan, W. Zhang, S. Duan, X. G. Zhao, and A. O. Govorov, Phys. Rev. B **77**, 165301 (2008).

[12] J.-Y. Yan, W. Zhang, S. Duan, and X. G. Zhao, J. Appl. Phys. **103**, 104314 (2008).

[13] K. Okamoto, I. Niki, A. Shvartser, Y. Narukawa, T. Mukai, and A. Scherer, Nat. Mater. **3**, 601 (2004).

[14] Y. Fedutik, V. V. Temnov, O. Schöps, U. Woggon, and M. V. Artemyev, Phys. Rev. Lett. **99**, 136802 (2007).

[15] J. S. Biteen, L. A. Sweatlock, H. Mertens, N. S. Lewis, A. Polman, and H. A. Atwater, J. Phys. Chem. C **111**, 13372 (2007).

[16] I. Gontijo, M. Boroditsky, E. Yablonovitch, S. Keller, U. K. Mishra, and S. P. DenBaars, Phys. Rev. B **60**, 11564 (1999).

[17] A. Neogi, C.-W. Lee, H. O. Everitt, T. Kuroda, A. Tackeuchi, and E. Yablonovitch, Phys. Rev. B **66**, 153305 (2002).

[18] P. Anger, P. Bharadwaj, and L. Novotny, Phys. Rev. Lett. **96**, 113002 (2006).

[19] S. A. Maier, M. L. Brongersma, P. G. Kik, S. Meltzer, A. A. G. Requicha, and A. Atwater, Adv. Mater. **13**, 1501 (2001).

[20] D. K. Gramotnev and S. I. Bozhevolnyi, Nat. Photonics **4**, 83 (2010).

[21] M. I. Stockman, Opt. Express **19**, 22029 (2011).

[22] P. Berini, Adv. Opt. Photon. **1**, 484 (2009).

[23] V. I. Sugakov and G. V. Vertsimakha, Phys. Rev. B **81**, 235308 (2010).

[24] H.-C. Wang, X.-Y. Yu, Y.-L. Chueh, T. Malinauskas, K. Jarasiunas, and S.-W. Feng, Opt. Express **19**, 18893 (2011).

[25] P. Vasa, R. Pomraenke, S. Schwieger, Y. I. Mazur, V. Kunets, P. Srinivasan, E. Johnson, J. E. Kihm, D. S. Kim, E. Runge, G. Salamo, and C. Lienau, Phys. Rev. Lett. **101**, 116801 (2008).

[26] A. Hatef, S. M. Sadeghi, and M. R. Singh, Nanotechnology **23**, 065701 (2012).

[27] R. D. Artuso, G. W. Bryant, A. Garcia-Etxarri, and J. Aizpurua, Phys. Rev. B **83**, 235406 (2011).

[28] A. Ridolfo, O. Di Stefano, N. Fina, R. Saija, and S. Savasta, Phys. Rev. Lett. **105**, 263601 (2010).

[29] M. R. Singh, D. G. Schindel, and A. Hatef, Appl. Phys. Lett. **99**, 181106 (2011).

[30] A. O. Govorov, Phys. Rev. B **82**, 155322 (2010).

[31] R. D. Artuso and G. W. Bryant, Phys. Rev. B **82**, 195419 (2010).

[32] A. Manjavacas, F. J. García de Abajo, and P. Nordlander, Nano Lett. **11**, 2318 (2011).

[33] S. M. Sadeghi, Phys. Rev. B **79**, 233309 (2009).

[34] M.-T. Cheng, S.-D. Liu, H.-J. Zhou, Z.-H. Hao, and Q.-Q. Wang, Opt. Lett. **32**, 2125 (2007).

[35] M.-T. Cheng, S.-D. Liu, and Q.-Q. Wang, Appl. Phys. Lett. **92**, 162107 (2008).

[36] A. O. Govorov and I. Carmeli, Nano Lett. **7**, 620 (2007).

[37] A. O. Govorov, G. W. Bryant, W. Zhang, T. Skeini, J. Lee, N. A. Kotov, J. M. Slocik, and R. R. Naik, Nano Lett. **6**, 984 (2006).

[38] J. Lee, P. Hernandez, J. Lee, A. O. Govorov, and N. A. Kotov, Nat. Mater. **6**, 291 (2007).

[39] Q. Zhang, X.-Y. Shan, X. Feng, C.-X. Wang, Q.-Q. Wang, J.-F. Jia, and Q.-K. Xue, Nano Lett. **11**, 4270 (2011).

[40] Y. Fedutik, V. Temnov, U. Woggon, E. Ustinovich, and M. Artemyev, J. Am. Chem. Soc. **129**, 14939 (2007).

[41] E. A. Muljarov, E. A. Zhukov, V. S. Dneprovskii, and Y. Masumoto, Phys. Rev. **62**, 7420 (2000).

[42] T. Kuykendall, P. Ulrich, S. Aloni, and P. D. Yang, Nat. Mater. **6**, 951 (2007).

[43] H. Ajiki, T. Kaneno, and H. Ishihara, Phys. Rev. B **73**, 155322 (2006).

[44] H. Ajiki, K. Takizawa, and K. Cho, J. Lumin. **87–89**, 341 (2000).

[45] H. Ajiki, T. Tsuji, K. Kawano, and K. Cho, Phys. Rev. B **66**, 245322 (2002).

[46] S. Glutsch, D. S. Chemla, and F. Bechstedt, Phys. Rev. B **54**, 11592 (1996).

[47] R. B. Liu and B. F. Zhu, Phys. Rev. B **66**, 033106 (2002).

[48] J.-Y. Yan, Phys. Rev. B **78**, 075204 (2008).

[49] J.-Y. Yan, R. B. Liu, and B. F. Zhu, New J. Phys. **11**, 083004 (2009).

[50] P. B. Johnson and R. W. Christy, Phys. Rev. B **6**, 4370 (1972).